Studying the effect of pyrolysis gas composition on the gasification syngas composition using CPFD simulation

Ahmad T. Dawod Britt M. E Moldestad Hildegunn H. Haugen Janitha C. Bandara

Department of Process, Energy and Environmental Technology, University of South-Eastern Norway, Norway,
ahmad.dawod93@hotmail.com {britt.moldestad, hildegunn.h.haugen, janitha.bandara}@usn.no

Abstract

A CPFD model for biomass gasification in a bubbling fluidized bed was developed using the Barracuda Virtual Reactor 17.4.1 commercial CFD code. Three simulation cases were performed at varying the reactor temperature and pyrolysis gas compositions. The effect of the pyrolysis step was found to be significant, especially on the production of CO, H_2, and CH_4. This is mainly because that the pyrolysis step converts 85% of the biomass weight into volatiles.

Comparing the simulation results with the experimental data showed a good agreement on predicting CH_4 and H_2, whereas CO_2 was overestimated, and CO was underestimated. This might be due to inaccuracies in the pyrolysis gas composition or high rates in the water-gas-shift reaction used in the simulation.

The effects of temperature on the synthesis gas composition were further investigated. Increasing the temperature from 800°C to 900°C, increased the concentration of CO and H_2 by 2.4% and 1.6% respectively, while decreased the concentration of CO_2 and CH_4 by 1.3% and 0.5%, respectively. The trends of gas compositions showed a good agreement with other literature data, except the trend of CH_4. This might be due to the neglect of tar composition in the volatiles.

Keywords: Pyrolysis, Biomass gasification, CPFD.

1 Introduction

Waste generation has increased greatly in the ongoing many years, and there are no signs of decline. 2.01 billion tons of municipal solid waste (MSW) is generated globally every year (Kaza *et al*., 2018). According to the World Bank estimation, the overall waste generation will increase by around 70% to 3.4 billion tons by 2050. This is due to various components, such as population growth, urbanization, economic development, and customer shopping habits (Ellis, 2018). At least 33% of the generated waste worldwide is not managed in an environmentally safe way and instead dumped or openly burned (Kaza *et al*., 2018).

Biomass resources, also known as bio-renewable resources, refer to all types of organic non-fossil materials, such as plant, animal, and waste materials (Luo & Zhou, 2012) (Alternativ Energy Tutorials, 2015). Biomass fuels are classified as environmentally friendly, and the use of biomass for energy production is on the rise. As a result, all available biomass resources are becoming increasingly important (Rosendahl, 2013).

1.1 Pyrolysis and gasification of biomass

Pyrolysis of biomass is one of the thermal treatment technologies that breaks biomass into bio-oil, solid biochar, and gases. Pyrolysis is defined as the breaking down of any solid (or liquid) hydrocarbon by heating to high temperatures in the absence of oxygen (Basu, 2013). Bio-oil from the pyrolysis is an increasing interest due to its economical storage and transportation compared to solid biomass, which can be alternative combustion fuel for power generation and transportation (Luo *et al*., 2012). Biochar has different industrial applications such as solid fuel in boilers and the production of activated carbon. Finally, the gas fraction can be used as a fuel for industrial combustion or in supplying the energy required for the pyrolysis process itself (Goyal *et al*., 2008).

Biomass gasification process, in contrast to pyrolysis, tends to maximize the gas fraction by rearranging the biomass molecular structure in the presence of a gasifying agent such as air, oxygen or steam (Rosendahl, 2013) (Basu, 2013). Biomass particles undergo a chain of conversion processes, which include drying, pyrolysis, combustion, and char gasification (Sun, 2014; Basu, 2013). The product gas mixture is called synthesis gas or syngas, which consists of CO_2, CO, CH_4, H_2, H_2O, and small amounts of heavier hydrocarbons (Monilo *et al*., 2016).

There are three types of reactors (gasifiers) used for biomass gasification: fixed or moving bed, fluidized bed, and entrained flow gasifiers. They differ mainly in their flow conditions, gas-solid contact mode, and residence time of biomass inside the reactors (Monilo *et al*., 2016; Badeau *et al*., 2009). Fluidized bed gasification reactors are characterized by effective temperature distribution and high mass and heat transfer rates compared to other reactor types (Rosendahl, 2013). The bed material (e.g., sand) inside the reactor act as a heat carrier and a mixing enhancer (Basu, 2013). The fluidized bed gasification reactors are classified into two types: bubbling fluidized beds and circulating fluidized

beds. They differ mainly in fluidized gas velocity and gas path (Gomez-Barea & Leckner, 2010).

1.2 CPFD simulations

The multiphase particle in cell (MP PIC) method is used in the Barracuda VR, which has found to be an efficient tool for the simulation of fluidized bed reactors and other gas particle processes. Barracuda VR is specialized CFD software that is commonly used for simulation and analysis of fluidized bed reactors and other gas-solid processes (CPFD, 2019). The software is competent in optimizing operational conditions, geometry, inlets and outlets, flow rates, and particle properties, where some of them is difficult to achieve with experiments (CPFD Software, 2021). This numerical approach solves the fluid phase with the Eulerian computational grid and models the solid phase with Lagrangian computational particles (Perera, 2013). A given number of particles having the same properties are expressed by parcels to minimize the computational costs (CPFD Software, 2021). The present work uses the Barracuda VR software for the simulation of the biomass gasification process.

1.3 Objectives

The overall aim was to simulate a fluidized bed gasification reactor using a computational particle fluid dynamic (CPFD) and using actual experimental data from pyrolysis as an input.

Another aim is to study the composition of the synthesis gas obtained from gasification of wood pellets and compare them with the experimental results performed at USN and conducted by Bandara (Bandara, 2021). Further, the aim is to study the effect of pyrolysis gas composition and reactor temperature on the synthesis gas composition.

2 Material and methods

The experimental works of a previous study was used for the comparison with the simulation results. The experimental method is discussed briefly, and further details were presented in previous publications (Bandara, 2021).

2.1 Experimental methods

The gasification experimental rig is a bubbling fluidized bed reactor with a fuel capacity of 20kW and is installed at the University of South-Eastern Norway. Figure 1 show a schematic diagram of the biomass gasification rig. The reactor has a diameter of 100mm and a height of 1000mm. Three electrical heaters are installed on the reactor wall which heats up the reactor during operation. The gasifying air is heated by an air heater before it flows into the reactor.

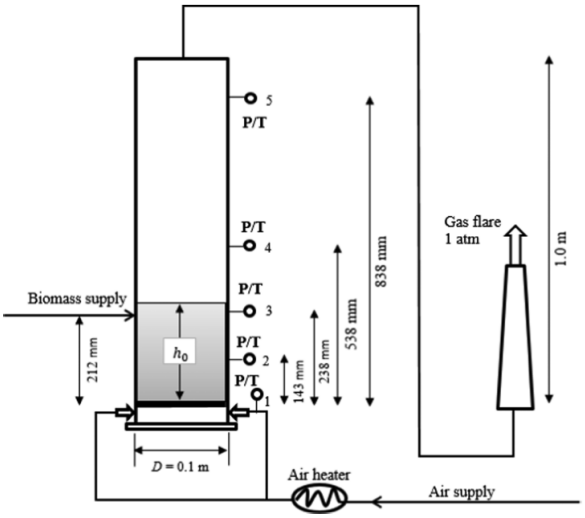

Figure 1. Schematic diagram of the biomass gasifier.

Temperature and pressure sensors are placed in different locations along the reactor height to measure the variation in pressure and temperature during the operation. The fuel is stored in a silo and supplied to the reactor using two screw conveyers. The bed material (sand) is supplied to the reactor from the funnel type opening placed at the reactor wall. A constant nitrogen flow of 0.5 L/min is maintained across the silo to avoid any gas leakages from the reactor to the silo. A sampling line is attached at the reactor outlet. A gas chromatograph (GC) SRI 8610C using helium as a carrier gas, is used to determine the gas composition fraction (O_2, N_2, CH_4, CO_2, and CO).

The experiments were carried out using wood pellets of 6 mm in diameter and 5-30 mm in length. The experiments were performed at USN and conducted by Bandara (Bandara, 2021).

2.2 CPFD methods

Computational particle fluid dynamic (CPFD) software was used to simulate the biomass gasification reactor. The Barracuda Virtual reactor (VR) version 17.4.1 software simulates multiphase hydrodynamics, heat balance, and chemical reactions of fluid-particle systems in three dimensions. The Lagrange approach is used for the particle phase, and the Eulerian approach is used for the gas phase. Pyrolysis data obtained from different studies were used as an input for the simulation.

It should be noted that the simulation was done using a square-sectioned geometry to avoid small and missing grid sections that can arise in a cylindrical-shaped geometry. According to the study done by (Bandara, 2021), at least one biomass particle should be able to fit within the cell to avoid computational errors. However, the geometry has the same cross-section area as the cylindrical geometry used in experiments.

This section discusses the simulation setup and procedure used in Barracuda software to establish the simulation model.

2.2.1 Mesh and geometry

For the simulation of biomass gasification in bubbling fluidized bed, a geometry with 8.83 cm square cross-section and 100 cm height was created using the SolidWorks software. Figure 2 shows the meshed geometry (Grid), initial bed material, dimension of the geometry, and the locations of transient data points.

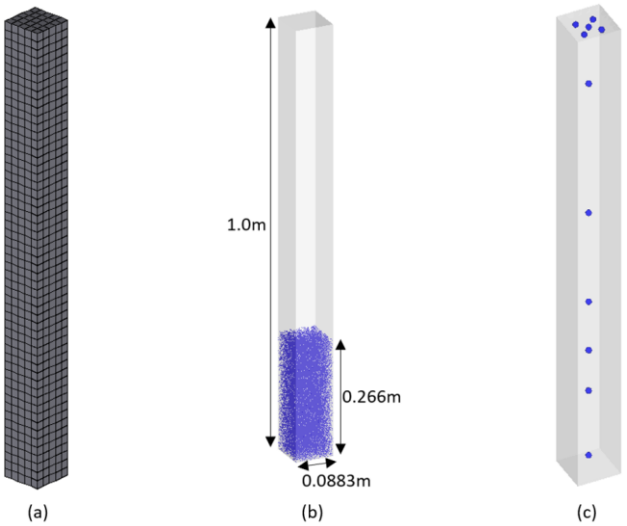

Figure 2. Simulation set-up: (a) Meshed geometry (b) Initial bed material and geometry dimensions (c) Transient data points.

As illustrated in Figure 2a, the simulated grid was generated with 6000 cells in total. Sand (SiO_2) particles with a mean diameter of 300µm and density of 2650 kg/m^3 were used as the bed material. The transient data points (sensors), as depicted in Figure 2c located along the center line of the reactor are used to measure the temperature and the pressure at different locations of the reactor, whereas datapoint located at the top surface measures the gas composition.

2.2.2 Initial and boundary conditions

The boundary conditions used in the geometry were specified as shown in Figure 3. Air was used as the gasification agent, which was implemented as a flow boundary. The syngas exit at the reactor top was a pressure boundary. The biomass inlet flow boundary was at 0.254m above the reactor bottom. Figure 3b shows the thermal boundary condition used to specify the constant temperature reactor wall, which was maintained by electrical heating elements during the experiments.

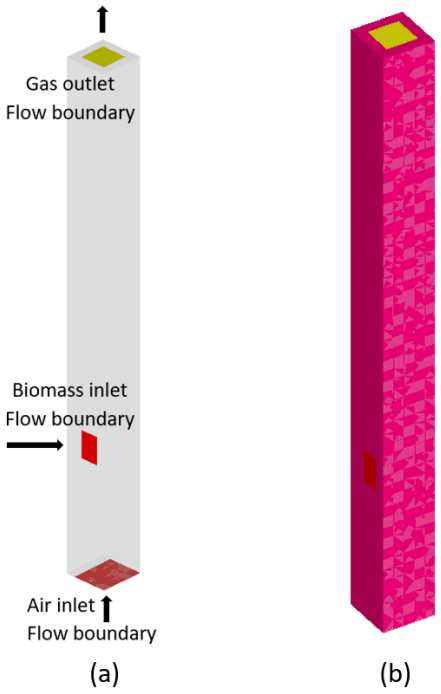

Figure 3. Boundary conditions: (a) Flow boundaries (b) Thermal boundary.

The reactor was initially filled with pure nitrogen at 1 atm and the temperature was varied according to the simulated case. The bed material is initially 100% sand (SiO_2) with a particle volume fraction of 0.6. The bed material was initially at 0.266 m height as illustrated in Figure 2b. depicted with blue color. The starting temperature was specified to be similar to the target operational temperature for all simulated cases.

2.2.3 Input data

Wen-Yu/Ergun drag model was adopted for the simulation as it was proven to give better predictions (Jaiswal, 2018). Table 1 shows the specified biomass properties, inlet flows, and simulation parameters used in the simulation.

Table 1. Biomass particle properties, inlet flows, and simulation parameters used in the simulation.

Biomass properties	
Type	Wood pellets (spherical shaped)
Size	2 mm
Inlet temperature	27°C (300K)
Density	1000 kg/m^3
Char density (after pyrolysis)	300 kg/m^3
Inlet flows	
Air	3 kg/h
Biomass	2.4 kg/h
Biomass carrier gas (N_2)	0.5 L/min
Air-Fuel ratio	1.25
Simulation parameters	
Close-pack volume fraction	0.6
Maximum momentum redirection from collision	40%
Normal-to-wall momentum retention coefficient	0.85
Tangent-to-wall momentum retention coefficient	0.85
Diffuse bounce	3
Drag model	Wen-Yu/Ergun

To define the wood pellets in the simulation software, the fraction of the volatiles and solid must be clarified. From the proximate analysis, wood pellets are broken into 83.9 wt.% volatiles, 15.55 wt.% fixed carbon, 0.55 wt.% ash, and 7.9 wt.% moisture in the pyrolysis stage. The amount of ash is very small; thus, the ash content was neglected. The moisture content was included in the volatile phase. Biomass char is considered to consist of pure carbon.

Hundreds of chemical reactions might occur in a gasification reactor. However, only the major reactions were considered, and the chemical kinetics are presented in Table 2.

Table 2. Chemical reactions and Kinetics for air gasification

Chemical reactions	Kinetics
Water gas shift reaction (Ismail *et al.*, 2019) R1: $CO + H_2O \leftrightarrow CO_2 + H_2$	$r = 6.4 \times 10^9 T \exp\left(\frac{-39{,}260}{T}\right)$
CO combustion (Gomez *et al.*, 2010) R2: $CO + 1/2O_2 \rightarrow CO_2$	$r = 4.78 \times 10^8 \exp\left(\frac{-6.69 \times 10^4}{RT}\right) [CO][O_2]^{0.3}[H_2O]^{0.5}$
H_2 combusion (Desroches *et al.*, 1998) R3: $H_2 + 1/2O_2 \leftrightarrow H_2O$	$r = 2.2 \times 10^9 \exp\left(\frac{-1.09 \times 10^5}{RT}\right) [H_2][0_2]$
Methane reforming (Kumar *et al.*, 2019) R4: $CH_4 + H_2O \leftrightarrow CO + 3H_2$	$r = 3.015 \times 10^8 \exp\left(\frac{-1.2552 \times 10^5}{RT}\right) [CH_4][H_20]$
Char oxidation (Kumar *et al.*, 2019) R5: $2C + O_2 \leftrightarrow 2CO$	$r = 1.47 \times 10^5 \exp\left(\frac{-1.13 \times 10^8}{RT}\right) [0_2]$
Steam gasification (Kumar *et al.*, 2019) R6: $C + H_2O \leftrightarrow CO + H_2$	$r = 8.28 \exp\left(\frac{-1.882 \times 10^8}{RT}\right) [H_2O]$
Boudouard reaction (Radmanesh *et al.*, 2006) R7: $CO_2 + C \leftrightarrow 2CO$	$r = 3.42\,T \exp\left(\frac{-15600}{T}\right) [C0_2]$

2.2.4 Simulation procedure

Three simulation cases were established by changing the reactor and pyrolysis temperatures. and fitting the pyrolysis gas compositions according to data from the literature. The specific data of pyrolysis gas composition for each case are tabulated in Table 3.

Table 3. Input data for the simulation cases (Santamaria, et al., 2021).

Case number	**Gas composition (wt.%)**					
	H_2O	H_2	CH_4	CO_2	CO	Tar (benzene)
Case-A	9	2	12	36	41	
Case-B	9	1	11	24	37	18
Case-C	9	2	12	36	41	

For Case-A, the reactor temperature was set to 800°C and the pyrolysis gas composition for 800°C was fitted. Case-B was modified by setting the reactor temperature to 800°C and fitting the pyrolysis gas composition for 700°C. It was assumed that if the mixing is not efficient

at the feeding point, the temperature can drop down to 700°C. In this case, the composition of tar (benzene) was included because pyrolysis yields more liquid at lower temperatures. Case-C is modified by increasing the reactor temperature up to 900°C and use the pyrolysis gas compositions for 800°C. The special aim of these cases was to study the effect of temperature and pyrolysis gas composition on biomass gasification. And thereby, compare the results with the experimental results from other studies performed at the USN gasification rig.

The total simulation time for each case was set to 200 seconds with a time step of 0.001 seconds. The gas compositions measured by the transient data points were averaged for the last simulated 100 seconds.

3 Results and discussion

This section discusses the simulation data for each case. The data were further compared against experiments.

3.1 Case-A

Case-A was modified by setting the reactor temperature to 800°C using the pyrolysis gas composition for 800°C. Figure 4 shows the mass fraction of product species at the reactor outlet plotted after 100s of simulated time. The average mass fraction of CO was 10.4%, CO_2 was 39.4%, CH_4 was 4.2% and H_2 was 1.1%.

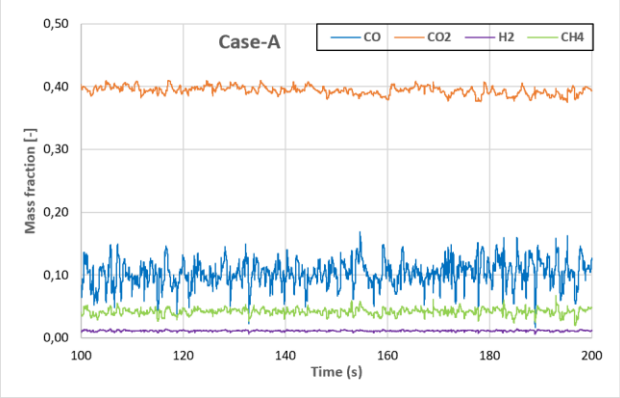

Figure 4. Case-A: Outlet mass fraction variation with time.

Figure 5 shows an outline of the (a) fluid temperature (b) particle temperature and (c) particle volume fraction across the bed at 200s. The fluid and particle temperatures are above 800°C (1073K), which is the desired temperature. This indicates that the gasification reactions are continuously maintained. From Figure 5c, the particles seem to be well mixed, which is good in terms of temperature distribution. The air flow might be a little bit high, but as long the particles remain within the bed it is accepted. However, limited air flows can reduce the generation of combustible gases such as CO, H_2, and CH_4.

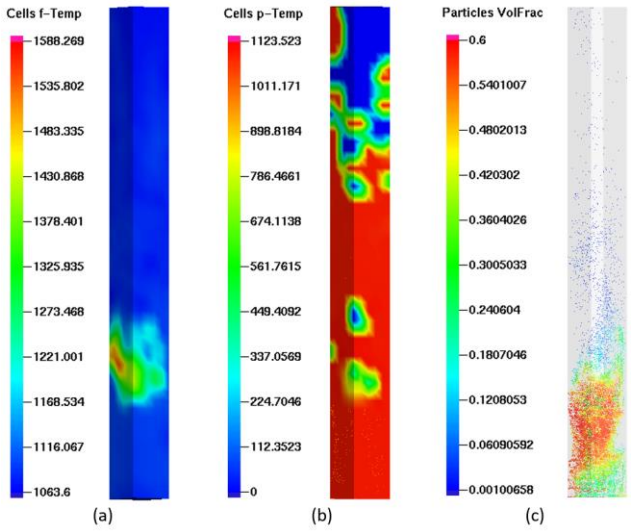

Figure 5. Reactor conditions (a) Fluid temperature [K] (b) Particle temperature (c) Particle's volume fraction.

3.2 Case-B

In Case-B, the reactor temperature was kept at 800°C and the pyrolysis gas composition for 700°C was fitted. Figure 6 shows the mass fraction of product species at the reactor outlet plotted after 100s of simulated time. The average mass fraction of CO was 13.2%, CO_2 was 32.4%, CH_4 was 4.1% and H_2 was 0.9%. As the pyrolysis gas composition for 700°C was fitted in this case, the tar content is significant. Thereby, the tar composition was modified within the volatiles and the tar reactions were included in the simulation. The tar was assumed by a single component, that is benzene C_6H_6.

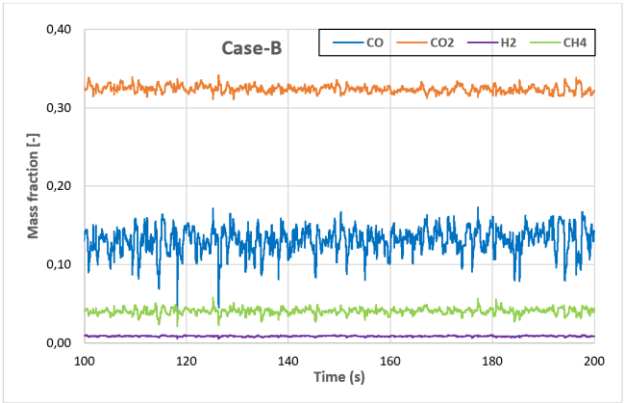

Figure 6. Case-B: Outlet mass fraction variation with time.

3.3 Case-C

Finally, Case-C was modified by setting the reactor temperature to 900°C and fitting the pyrolysis gas composition for 800°C. Figure 7 shows the mass fraction of product species at the reactor outlet plotted after 100s of simulated time. The average mass fraction of CO was 13.1%, CO_2 was 37.9%, CH_4 was 3.9% and H_2 was 1.2%.

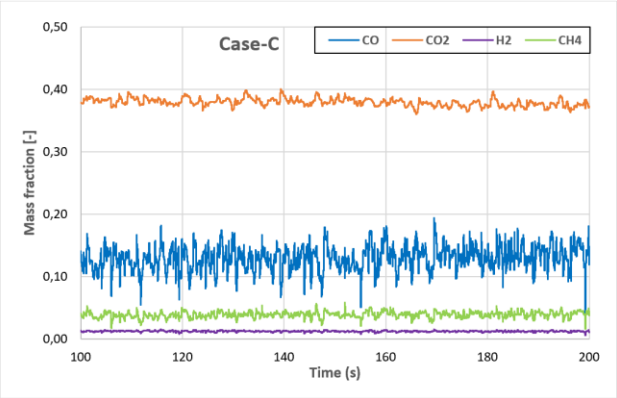

Figure 7. Case-C: Outlet mass fraction variation with time.

From Figure 4, Figure 6, and Figure 7, the calculated product mass fractions are showing a noisy and unsteady behavior where, the steady-state is never reached. This is due to the unsteady characteristics of the fluidized bed, where different chemical and physical transformations are taking place. However, it was noticed from the plots that the average mass fractions were stable over time.

3.4 Comparison of the cases

The molar compositions of the syngas from simulations and experiments at 800°C is given in Figure 8 and Table 4. In all cases, N_2 contributed to the highest molar concentration and ranged between 41.5% and 43.5% of the total. This is reasonable, as nitrogen is an inert gas and does not involve in the reactions. The molar concentrations of O_2 were monitored to be very close to zero. This is mainly due to the occurrence of oxidation reactions. The H_2O molar concentrations were measured to be 2.5%, 1.6%, and 1.2% for Case-A, B, and C, respectively. The lower percentage of H_2O produced in Case-C is mainly due to the increase of temperature to 900°C. Higher temperatures enhance the steam gasification reaction (R6) to proceed forward, which in turn produces more H_2. In all cases, the molar concentration of CO_2 was highest followed by H_2 and CO, respectively. The lowest produced gas component was CH_4.

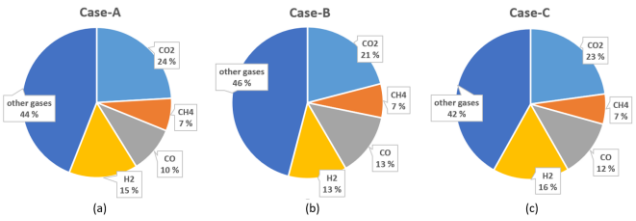

Figure 8. Molar compositions of the gas species monitored at the reactor outlet for (a) Case-A (b) Case-B (c) Case-C.

Case-A and Case-B were simulated using the same reactor temperature but different pyrolysis gas compositions. Therefore, the results from the two cases are compared to study the effect of the pyrolysis step. Figure 9 and Figure 10 show the input pyrolysis gas compositions for Case-A and B respectively, compared to the synthesis gas compositions.

The molar concentration of CO_2 increased slightly by 3% and 2.6% in the synthesis gas for Case-A and B, respectively. In the contrast, the CO concentration decreased significantly by 27% and 29.9% in the synthesis gas for Case-A and B, respectively. The concentration of CH_4 decreased by 6.9% and 7.1% in the synthesis gas for Case-A and B, respectively. The concentration of H_2 decreased by 8.2% and 4.7% in the synthesis gas for Case-A and B, respectively.

The increase of CO_2 is mainly due to the oxidation of char and CO in the gasifier. Oxidation and water gas shift reaction (R1) are the main drives for the reduction of CO. Consumption of methane is mainly due to steam methane reforming reaction (R4), which is in turn produces more CO.

It was observed that higher concentrations of the combustible gases including CH_4, CO, and H_2 released in the pyrolysis stage contributed to higher concentrations of these gases in the synthesis gas. Therefore, pyrolysis stage is critical in deciding how much CH_4, CO, and H_2 will be in the synthesis gas. This is mainly because that the pyrolysis step converts 85% of the biomass weight into volatiles.

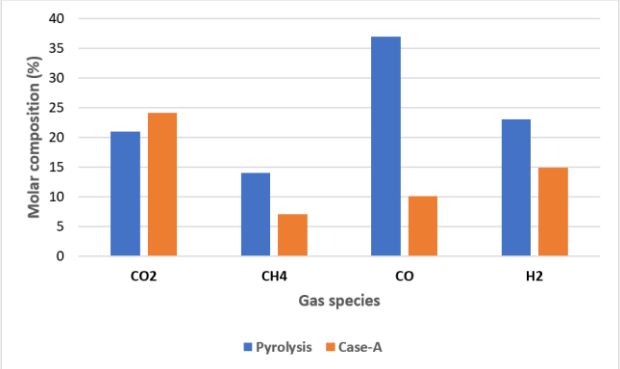

Figure 9. Case-A: Input pyrolysis gas composition compared to synthesis gas composition.

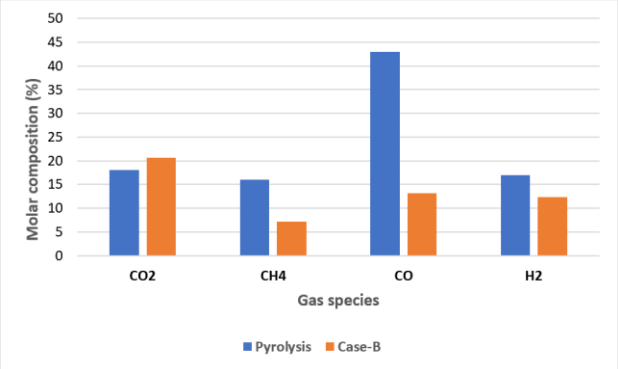

Figure 10. Case-B: Input pyrolysis gas composition compared to synthesis gas composition.

Figure 11 shows the average gas compositions from the simulation of Case-A and B compared with the

experimental results. It should be noted that only Case-A and B are comparable with the experimental results, as they have the same reactor temperature. Both cases show a good agreement with the experimental results for CH_4 and H_2. Case-B gave a closer prediction on CO_2 and CO, which is not as expected because Case-B uses the pyrolysis gas composition for 700°C. This might be due to the tar that was defined in Case-B. However, in both cases, the concentration of CO_2 was overestimated, CO was underestimated while CH_4 was slightly overestimated.

The overestimation of CO_2 and underestimation of CO might be due to some inaccuracies in the pyrolysis gas composition or high rates in the water-gas-shift reaction (R1) where CO is consumed, and more CO_2 is produced. Moreover, there can also be some experimental uncertainties in measuring the gas composition, especially related to the GC measurements and the gas sampling. During the experiment, biomass feeding was not continuous in contrast to the simulation. As the pyrolysis gas composition highly affects the final syngas composition, discontinuous feeding might cause deviations in the actual measured value. In the simulation, it is possible to take a wide range of measurements, which is difficult during the experiments.

However, the deviation between experiment and simulation cannot be avoided. This is mainly because the reaction network is decreased, devolatilization is simplified and the tar generation is minimized or ignored.

Table 4. Average gas composition (mole basis) from the simulated cases and experiment.

	Case-A	Case-B	Case-C	Experiment
CO_2	24.1	20.6	22.82	14
CH_4	7	7.1	6.5	4
CO	10	13.1	12.4	19
H_2	14.8	12.3	16.4	17

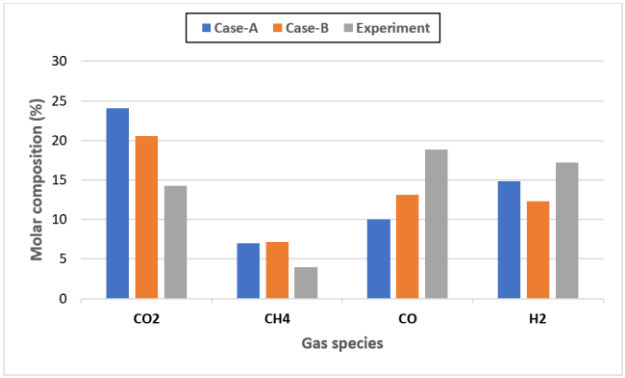

Figure 11. Average product gas composition from the three cases compared to the experimental results.

Case-A and C are compared with each other to study the effect of temperature on the synthesis gas composition. Two cases are defined with the same pyrolysis gas composition but with different temperatures. Figure 12 shows the product gas composition from Case-A and Case-B with varying reactor temperature. Increasing the temperature from 800°C to 900°C, the CO molar concentration increased from 10% to 12.4%, CO_2 decreased from 24.1% to 22.8%, CH_4 decreased slightly from 7% to 6.5% and H_2 increased from 14.8% to 16.4%. This is mainly due to the reactions that are enhanced with increasing temperature including, char partial oxidation reaction (R5), water gas shift reaction (R1), and the Boudouard reaction (R7). Further, the reactor temperature has a significant effect on the syngas product yields. Therefore, increasing the reactor temperature contributes to higher gas composition and lower tar yields. However, the trends show a good agreement with literature and other experiments except for the trend of CH_4. This might be due to the neglect of the tar composition in the volatiles.

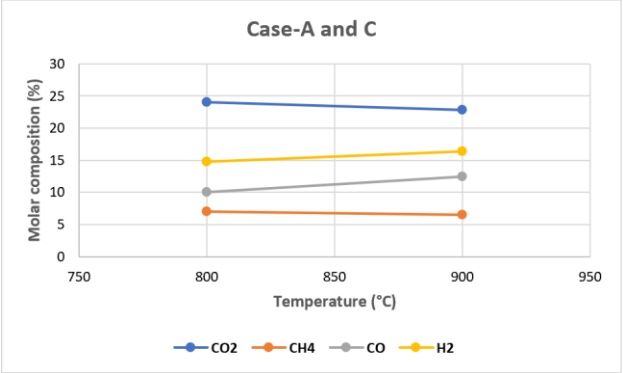

Figure 12. Product gas molar fraction for Case-A and Case-C at different temperatures.

4 Conclusion

Computational particle fluid dynamic (CPFD) simulations were carried out to study the composition of the synthesis gas obtained from the air gasification of wood pellets. Three simulation cases were created by varying the temperature and the pyrolysis gas compositions.

In all the cases, production of CO_2 was highest, and then come H_2, CO, and CH_4, respectively. The effect of the pyrolysis step on synthesis gas composition was found to be significant, especially on the production of CO, H_2, and CH_4. This is mainly due to the 85% by weight of the synthesis gas was produced during the pyrolysis of biomass.

Comparing Case-A and B with experimental data showed a good agreement on predicting CH_4 and H_2 while overestimation of CO_2 and underestimation of CO. The deviation of CO_2 and CO might be due to uncertainty in the pyrolysis gas composition or high kinetic rates of water-gas shift reaction used in the simulation. Including the decomposition of tar in the simulation seems to give better prediction performance, especially for CO_2 and CO.

The effect of temperature was established by comparing Case-A and C, where the temperature was varied from 800°C up to 900°C. Increasing the temperature increased the concentration of CO and H_2 by 2.4% and 1.6% respectively and decreased the concentration of CO_2 and CH_4 by 1.3% and 0.5%. The trends showed a good agreement with other experiments from the literature, except the trend of CH_4. This might be due to the neglect of the tar compositions in the volatiles.

References

Alternativ Energy Tutorials. *Biomass Resources*. Retrieved 03 2021, from https://www.alternative-energy-tutorials.com/biomass/biomass-resources.html

J.P. Badeau, A. Levi. *Biomass Gasification: Chemistry, Processes and Applications.* New York: Nova Science Publishers. 2009.

J. Bandara. *Simulation and parameter optimization of fluidized-bed and biomass gasification.* University of South-Eastern Norway, 2021.

P. Basu. *Biomass Gasification, Pyrolysis and Torrefaction* (2nd ed.). Elsevier, 2013.

CPFD Software. *Complements Other Tools*, 2021. Retrieved from https://cpfd-software.com/technology/complements-other-tools/

CPFD Software LLC. *CPFD Software Realeases Barracuda Virtual Reactor 17.4*. Retrieved 05.03.2021: https://cpfd-software.com/news/cpfd-software-releases-barracuda-virtual-reactor-17.4

E. Desroches-Ducarne, J. C.Dolignier, E. Marty, G. Martin, L. Delfosse. Modeling of gaseous pollutants emissions in circulating fluidized bed combustion of municipal refuse. *Fuel*, 77(13): 1399-1410, 1998.

C. Ellis. *World Bank: Global waste generation could increase by 70% by 2050.* World Bank: Global waste generation could increase 70% by 2050 | Waste Dive, Industry Dive 2018.

L. Fagbemi, L. Khezami, R. Capart. Pyrolysis products from different biomasses: application to the thermal cracking of tar. *Applied Energy*, 69(4), 293-306, 2001.

A. Gomez-Barea, B. Leckner. Modeling of biomass gasification in fluidized bed. *Progress in Energy and Combustion Science*, 36(4): 444-509, 2010.

H. B. Goyal, D. Seal, R. C. Saxena. Bio-fuel from thermochemical conversion of renewable resources: A review. *Elsevier*, 12(2): 504-517, 2008.

M. T. Ismail, A. Ramos, M. A. El-Salam, E. Monteiro, A. Rouboa. Plasma fixed bed gasification using a Eulerian model. *International Journal of Hydrogen Energy*, 44(54): 28668-28684, 2019.

R. Jaiswal, R. *Computational modeling and experimental studies on fluidized bed regimes.* University of South-Eastern Norway, 2018.

S. Kaza, L. Yaw, P. Bhada-Tata, F. V. Woerden. *What a Waste.* Washington: International Bank for Reconstruction and development. 2018.

U. Kumar, M. C. Paul. CFD modeling of biomass gasification with a volatile break-up approach. *Chemical Engineering Science, 195*: 413-422, 2019, doi: https://doi.org/10.1016/j.ces.2018.09.038

Z. Luo, J. Zhou. Thermal Conversion of Biomass. *Handbook of Climate Change Mitigation*: pp. 1001-1042. New York: Springer, 2012.

A. Monilo, S. Chianese, D. Musmarra. Biomass gasification technology: The state of the art overview. *Journal of Energy Chemistry*, 25(1): 10-25, 2016.

C. K. Perera, *Optimization of biomass gasification reactor.* Telemark University College, 2013.

R. Radmanesh, J. Chaouki, C. Guy. Biomass gasification in a bubbling fluidized bed reactor: Experiments and modeling. *AIChE Journal*, 52(12): 4258-4272, 2006. doi: https://doi.org/10.1002/aic.11020

L. Rosendahl. *Biomass Combustion Science, Technology and Engineering.* Sawston: Woodhead Publishing Limited, 2013.

L. Santamaria, M. Beirow, F. Mangold, G. Lopez, M. Olazar, M. Schmid, G. Scheffknecht. Influence of temperature on products from fluidized bed pyrolysis of wood and solid recovered fuel. *Fuel*, 283, 2021.

K. Sun. *Optimization of biomass gasification reactor using Aspen Plus.* Telemark University College. 2014.